Assessment of the efficiency of long-range corrected functionals for some properties of large compounds

Denis Jacquemin[a),b)] and Eric A. Perpète
Laboratoire de Chimie Théorique Appliquée, Facultés Universitaires Notre-Dame de la Paix, rue de Bruxelles, 61, B-5000 Namur, Belgium

Giovanni Scalmani and Michael J. Frisch
Gaussian, Inc., Wallingford, Connecticut 06492

Rika Kobayashi
ANU Supercomputer Facility, Leonard Huxley Building 56, Canberra, Australian Capital Territory 0200, Australia

Carlo Adamo[a),c)]
Ecole Nationale Supérieure de Chimie de Paris, Laboratoire Electrochimie et Chimie Analytique, UMR CNRS-ENSCP No. 7575, 11, rue Pierre et Marie Curie, F-75321 Paris Cedex 05, France

(Received 18 January 2007; accepted 16 February 2007; published online 11 April 2007)

Using the long-range correction (LC) density functional theory (DFT) scheme introduced by Iikura *et al.* [J. Chem. Phys. **115**, 3540 (2001)] and the Coulomb-attenuating model (CAM-B3LYP) of Yanai *et al.* [Chem. Phys. Lett. **393**, 51 (2004)], we have calculated a series of properties that are known to be poorly reproduced by standard functionals: Bond length alternation of π-conjugated polymers, polarizabilities of delocalized chains, and electronic spectra of extended dyes. For each of these properties, we present cases in which traditional hybrid functionals do provide accurate results and cases in which they fail to reproduce the correct trends. The quality of the results is assessed with regard to experimental values and/or data arising from electron-correlated wave function approaches. It turns out that (i) both LC-DFT and CAM-B3LYP provide an accurate bond length alternation for polyacetylene and polymethineimine, although for the latter they decrease slightly too rapidly with chain length. (ii) The LC generalized gradient approximation and MP2 polarizabilities of long polyphosphazene and polymethineimine oligomers agree almost perfectly. In the same way, CAM-B3LYP corrects the major part of the B3LYP faults. (iii) LC and CAM techniques do not help in correcting the nonrealistic evolution with chain length of the absorption wavelengths of cyanine derivatives. In addition, though both schemes significantly overestimate the ground to excited state transition energy of substituted anthraquinone dyes, they provide a more consistent picture once a statistical treatment is performed than do traditional hybrid functionals.
 [DOI: 10.1063/1.2715573]

I. INTRODUCTION

In the last two decades, density functional theory (DFT) and time-dependent density functional theory (TD-DFT) have been extensively used to model the static and dynamic properties of countless chemical structures.[1] To reach high-quality results, it is essential to select an adequate functional. Exchange-correlation functionals have been classified according to a ladder of increasing complexity,[1] whose three lowest rungs are local density approximation (LDA), generalized gradient approximation (CGA), and meta-GGA (including the Laplacian of the density and/or the *kinetic energy density*). However, even the most refined meta-GGA functional does not provide accurate results (or constant errors) for all the physicochemical properties. In fact, it appeared that the meta-GGA did not relieve the main weaknesses of GGA. Several years ago, Becke proposed to include a fraction of exact [i.e., Hartree-Fock (HF)] exchange in the functional, leading to the fourth rung of the ladder. Since the HF approach often yields errors opposite to those obtained at DFT level, the net result is a nearly systematic error-compensation phenomenon. This led to the well-known B3LYP model,[2] that 13 years after its creation, probably remains the most-used *ab initio* scheme in computational chemistry. While a few hybrids[3–5] have been designed on the basis of purely theoretical considerations,[1,6] the percentage of exact exchange included in most hybrids has been (semi)empirically determined, i.e., inputs from selected experiments have been used: like heats of formation, ionization potentials, electroaffinities, and geometrical parameters for small gas-phase molecules.[2,7–14] As a result of the variety of molecules and properties included in the training set, the fraction of exact exchange in "fitted" hybrid functionals considerably varies: from 10% for TPSSh (Ref. 11) to 44% for MPWB1K.[15] Of course, one could switch from one functional to another with respect to the property and system

[a)]Authors to whom correspondence should be addressed.
[b)]Electronic mail: denis.jacquemin@fundp.ac.be. URL: http://perso.fundp.ac.be/~jacquemd
[c)]Electronic mail: carlo-adamo@enscp.fr

investigated, but such an approach cannot be regarded as completely satisfying. In addition, despite its incredible success, DFT and, consequently, its TD-DFT counterpart encounter problems that seem (almost) independent of the form of the functional. The difficulties mainly occur in reproducing the experimental evolution of a series of properties while increasing the molecular size, especially for π-conjugated structures. Though additional troubles do also appear for interacting molecules (van der Waals complexes), three major (and probably the simplest) single-molecule cases illustrate usual (TD-)DFT failures: (i) Pure hybrids, even meta-GGA, cannot reproduce the bond length alternation (BLA, the difference between single and double bond lengths) in several conjugated polymers.[16–19] Sometimes, the description provided by hybrid functionals is more realistic, but this cannot be guaranteed.[20] (ii) The dipole moment, polarizabilities, and hyperpolarizabilities of conjugated chains do not correctly evolve with increasing molecular size in π-delocalized compounds such as the prototype polyacetylene (PA) oligomers and the errors can be of an order of magnitude, even with hybrids.[21,22] (iii) The electronic transitions are incorrectly described in charge-transfer structures, leading to large errors in transition energies, as well as ghost states.[23–26] In some ways, all these three problems are related to the so-called shortsightedness of DFT functionals: the density is not influenced by a change in the vicinal electronic distribution.[21,25,26] Of course, the use of optimal hybrids and very diffuse basis sets can help in attenuating these misleading trends, but they are unable to fully solve the problem in a consistent way. To improve DFT performance a series of attempts has been recently made based on physically sound approaches.[27–51] (i) One can correct the well-known self-interaction problem of DFT procedures. One of the most common approaches to solve this problem rests on the method proposed by Krieger *et al.* in 1992.[35] Unfortunately, the Krieger-Li-Iafrate (KLI) procedure involves orbital dependency of the functional itself and is consequently computationally demanding. A more tractable procedure is the averaged-density self-interaction correction (ADSIC) scheme,[37,39] that has been shown to provide BLA of PA oligomers in better agreement with MP2 results than pure DFT functionals.[27] (ii) Current TD-DFT,[36,38] that explicitly includes the current density in its formalism, is able to reproduce second-order Møller-Plesset polarizabilities for increasingly long compounds (but hydrogen chains).[40] (iii) It is possible to use optimized effective potential for exact exchange.[52] This elegant, though computationally involved, approach has been successfully applied to simulate the (hyper)polarizabilities of conjugated chains by Bulat and co-workers.[32,47] (iv) One can build functionals accounting for long-range (LR) effects by the addition of a growing fraction of exact exchange when the distance increases (see Sec. II).[29,30,33,34,41,42,44–46,48,49,51,53–55] This procedure has been originally developed by Savin,[41,42,45] modified and applied to several molecular properties by Hirao *et al.* (LC: long-range corrected functional)[29,30,33,34,54] and Handy *et al.* (CAM-B3LYP: Coulomb-attenuating method–B3LYP).[44,46,48] The performance of these LR functionals has been mostly evaluated for small molecules (G1, G2, or G3 set or the like).[44,46,48,49,51] For these systems, the quality of the results is comparable to the traditional hybrids.[29,33,44,48,49,51] To the best of our knowledge, there are only a few published applications for the "problematic" cases listed above: the computation of polarizabilities of oligoenes (LC and CAM),[33,53,56] a determination of the band gap in carbon nanotube (LC),[49] an extensive (hyper)polarizability computation for large push-pull chromophores (LC),[30] the calculation of transition energies for three medium size molecules in Ref. 34 (LC), the evaluation of charge-transfer state in bacteriochlorin, porphyrins and chlorophylls (CAM),[55,57] and tetrathiafulvalene diquinone (LC),[51] as well as the calculation of two-photon cross sections (LC and CAM).[53] From these previous studies, one can conclude that LR-DFT is efficient for computing polarizabilities and hyperpolarizabilities of PA and its substituted derivatives, and that the effect of CAM on transition energies is non-negligible, leading to a notably better agreement for the very large molecules treated in Ref. 55. However, no computation of the BLA nor extensive comparison with experimental electronic spectra of dyes of chemical interest has been performed yet.

In this contribution, we apply LC-DFT, combined to two functionals, and CAM-B3LYP to the three problematic properties (bond length alternation, polarizability, absorption spectra) of large molecular systems. In each case, we have selected at least two structures: one for which the traditional hybrid functionals satisfactorily correct the pure functionals, and another one for which both pure and full-range exchange hybrids are inadequate. This paper is organized as follows. In Sec. II, we summarize the LC and CAM equations and we detail our computational procedure. In Sec. III, we analyze the results obtained for the BLA of PA and polymethineimine (PMI) oligomers (Sec. III A), for the polarizability of polyphosphazene (PPh) and PMI chains (Sec. III B), and for the absorption spectra of anthraquinone (AQ) and cyanine (CYA) dyes (Sec. III C). All these systems are depicted in Fig. 1.

II. METHODOLOGY

A. Long-range corrections

As this contribution is mainly focused on the effect of the LC-GGA and CAM-B3LYP approaches, it is worth to outline the underlying theories. In the following, we use LR-DFT as a generic name for both LC-GGA and CAM-B3LYP. In the LC scheme,[29,30,33,34] the electron repulsion operator $1/r_{12}$ is split into a short-range and a long-range part by using the standard error function scheme originally proposed by Savin and Gill *et al.*[41,42,58]

$$\frac{1}{r_{12}} = \frac{1-\mathrm{erf}(\mu r_{12})}{r_{12}} + \frac{\mathrm{erf}(\mu r_{12})}{r_{12}}, \tag{1}$$

with μ a damping parameter. This straightforwardly leads to the partitioning of the total exchange term into short and long-range contributions:

$$E_x = E_x^s + E_x^l, \tag{2}$$

in which the LR contribution to the exchange is computed with HF integrals:

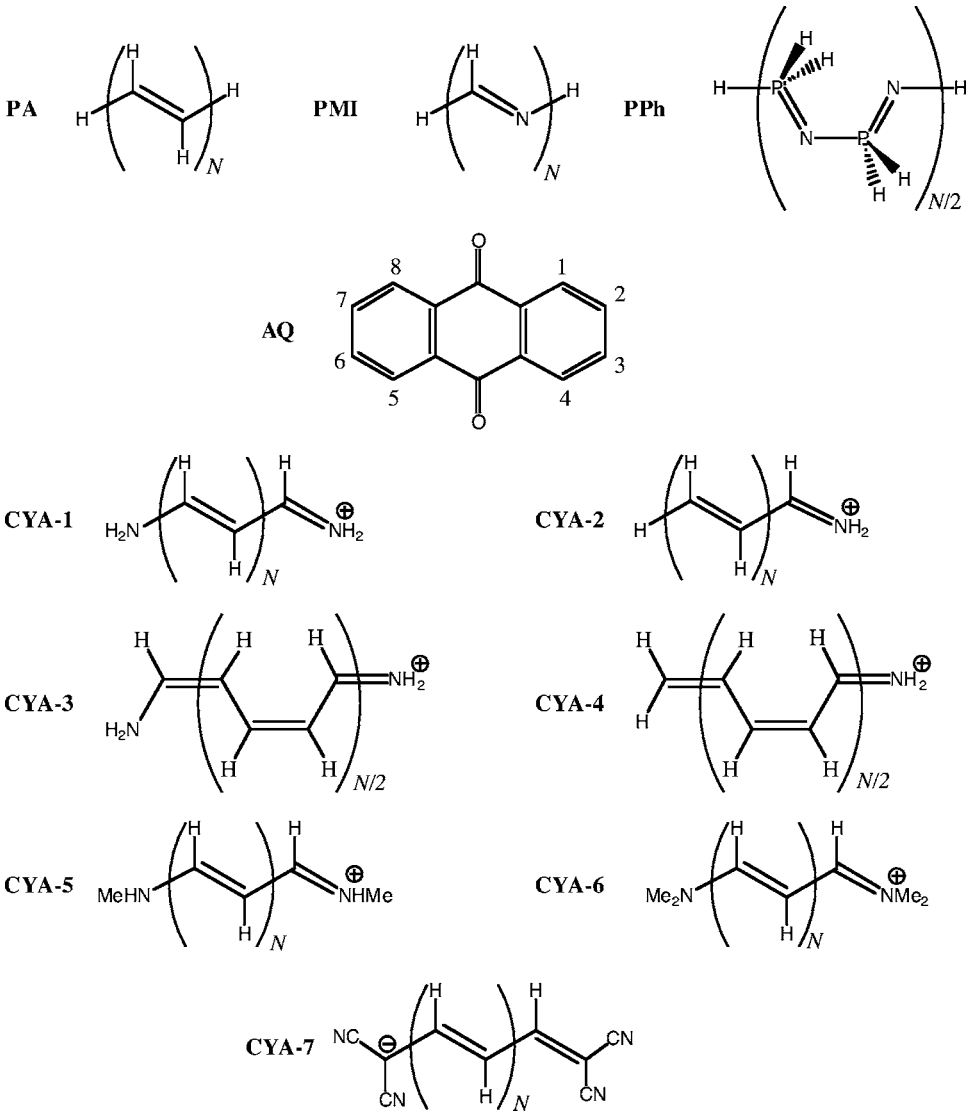

FIG. 1. Representation of the compounds investigated here. PA stands for polyacetylene, PMI for polymethineimine (all-*trans* conformer shown), PPh for polyphosphazene, AQ for anthraquinone, and the CYA-X are the several cyanine dyes considered.

$$E_x^l = -\sum_i^{\text{occ}} \sum_j^{\text{occ}} \left\langle \phi_i \phi_j \left| \frac{\text{erf}(\mu r_{12})}{r_{12}} \right| \phi_j \phi_i \right\rangle, \tag{3}$$

where ϕ are the molecular orbitals. The short-range contribution is a modified GGA functional that takes the form

$$E_x^s = -\sum_\sigma \int \rho_\sigma^{4/3} K_\sigma \left\{ 1 - \frac{8}{3} a_\sigma \left[\sqrt{\pi}\, \text{erf}\left(\frac{1}{2a_\sigma} \right) + 2a_\sigma (b_\sigma - c_\sigma) \right] \right\} d\mathbf{r}, \tag{4}$$

where ρ_σ represents the density of electron with spin σ at point $\mathbf{r}$ and K_σ is the enhancement factor. In Eq. (4), a_σ, b_σ, and c_σ are defined as

$$a_\sigma = \frac{\mu K_\sigma^{1/2}}{6\sqrt{\pi}\rho_\sigma^{1/3}}, \tag{5}$$

$$b_\sigma = \exp\left(-\frac{1}{4a_\sigma^2} \right) - 1, \tag{6}$$

$$c_\sigma = 2a_\sigma^2 b_\sigma + \frac{1}{2}. \tag{7}$$

Details regarding the computation of these terms can be found in Refs. 29, 30, 33, and 34.

In the CAM procedure of Yanai *et al.*[44] Eq. (1) is generalized by using two extra parameters (α and β),

$$\frac{1}{r_{12}} = \frac{1 - [\alpha + \beta\, \text{erf}(\mu r_{12})]}{r_{12}} + \frac{\alpha + \beta\, \text{erf}(\mu r_{12})}{r_{12}}. \tag{8}$$

In Eq. (8), $0 \leqslant \alpha + \beta \leqslant 1$, $0 \leqslant \alpha \leqslant 1$, and $0 \leqslant \beta \leqslant 1$ are three conditions to be satisfied. Within this formalism, LC-DFT corresponds to $\alpha = 0.0$ and $\beta = 1.0$, whereas B3LYP (Ref. 2) uses $\alpha = 0.2$ and $\beta = 0.0$ (in fact, as shown in Ref. 48, B3LYP is not *exactly* CAM-B3LYP with $\beta = 0.0$ and $\alpha = 0.2$ but the models are closely connected). Finally, the LR exchange writes[48]

$$E_x^l = \alpha E_x^{\text{HF}} - \beta \sum_i^{\text{occ}} \sum_j^{\text{occ}} \left\langle \phi_i \phi_j \left| \frac{\text{erf}(\mu r_{12})}{r_{12}} \right| \phi_j \phi_i \right\rangle, \tag{9}$$

with E_x^{HF} the exact exchange. The short-range contribution takes a form similar to Eq. (4):

TABLE I. 6-31G(*d*) BLA in the central unit cell of all-*trans* polyacetylene chains. The KLI and ADSIC calculations use a DZP basis set (see Ref. 27). All results are given in Å. *N* is the number of unit cells, i.e., the number of CH=CH units (Fig. 1).

		N								
Method		2	4	6	8	10	12	14	16	Ref.
Ψ	HF	0.1450	0.1281	0.1239	0.1227	0.1223	0.1221	0.1221	0.1221	19
	MP2	0.1138	0.0864	0.0756	0.0700	0.0669	0.0652	0.0642	0.0636	74
	CCSD	0.1233	0.1061	0.1017	0.1003					This work
	CCSD(T)	0.1154	0.0941	0.0880						This work
GGA	BLYP	0.1090	0.0713	0.0558	0.0471	0.0413	0.0372	0.0341	0.0318	19
	PBE	0.1052	0.0678	0.0528	0.0441	0.0385	0.0345	0.0316	0.0293	19
LR	LC-BLYP	0.1294	0.1099	0.1046	0.1028	0.1021	0.1017	0.1017	0.1016	This work
	LC-PBE	0.1262	0.1063	0.1009	0.0991	0.0982	0.0979	0.0978	0.0977	This work
	CAM-B3LYP	0.1267	0.1031	0.0958	0.0928	0.0914	0.0907	0.0904	0.0902	This work
SIC	ADSIC-LDA		0.085	0.065	0.053					27
	KLI-LDA		0.079	0.067	0.058					27
	ADSIC-PBE		0.089	0.066	0.056					27
Hybrids	B3-LYP	0.1169	0.0853	0.0730	0.0667	0.0628	0.0604	0.0587	0.0576	19
	PBE0	0.1157	0.0852	0.0739LYP	0.0680	0.0646	0.0624	0.0610	0.0601	19

$$E_x^s = -\frac{1}{2}\sum_\sigma \int \rho_\sigma^{4/3} K_\sigma \left\{ (1-\alpha) - \frac{8\beta}{3} a_\sigma \left[\sqrt{\pi}\,\mathrm{erf}\left(\frac{1}{2a_\sigma}\right) + 2a_\sigma(b_\sigma - c_\sigma) \right] \right\} d\mathbf{r}, \quad (10)$$

We refer interested readers to Refs. 44, 48, and 53 for further details.

B. Computational details

As we aim to assess the efficiency of the LR-DFT approach in challenging situations, we have selected cases for which reference values, either experimental or high-order electron correlation, do exist in the literature. For this reason, several Pople basis sets have been used. As the LC-DFT scheme mixes HF and DFT levels, it is reasonable to state that the basis set effects would not differ from the expected HF and DFT trends with respect to the extension of the atomic basis set. We have used two of the most popular GGA: BLYP and PBE. BLYP uses Becke's exchange[59] and Lee-Yang-Parr (LYP) correlation,[60] whereas PBE is based on Perdew-Burke-Ernzerhof for both exchange and correlation.[61] The most well-known hybrids built on these GGA have also been included: on the one hand, B3LYP,[2] a three parameter functional in which the exchange is a combination of 20% HF, Slater functional, and Becke's GGA correction, whereas the correlation part combines local and LYP functionals. On the other hand, PBE0 (Refs. 3 and 4) presents an exchange weighted (75% DFT/25% HF) accordingly to theoretical considerations.[6]

All calculations have been performed with the GAUSSIAN03 suite of programs,[62] except for the LC-DFT and CAM-B3LYP calculations that were carried out with a development version of GAUSSIAN.[63] The Coulomb-attenuating parameter μ in LC and CAM is set to the standard 0.33 value in the present work, whereas for CAM, the parameters α=0.19 and β=0.46 of Yanai *et al.*[44] are used. For all calculations, the self-consistent-field convergence criteria have been tightened to at least 10^{-8} a.u. and all geometry optimizations have been performed until the residual mean force is smaller than 1.0×10^{-5} a.u. (TIGHT threshold in GAUSSIAN).

For BLA computations, the most accurate integration grid [*ultrafine*, pruned (99,590) grid] has been chosen in order to be consistent with previous *ab initio* works.[19,20,64,65]

The static electronic polarizabilities (α) have been evaluated on the geometries described in the literature. In quasilinear chains, the longitudinal component of the α tensor (α_L) dominates the total response for sufficiently long chains and we consistently report this component only. The DFT α_L have been computed with the fully analytic coupled-perturbed Kohn-Sham approach. The α_L per unit cell have been obtained by using the relation

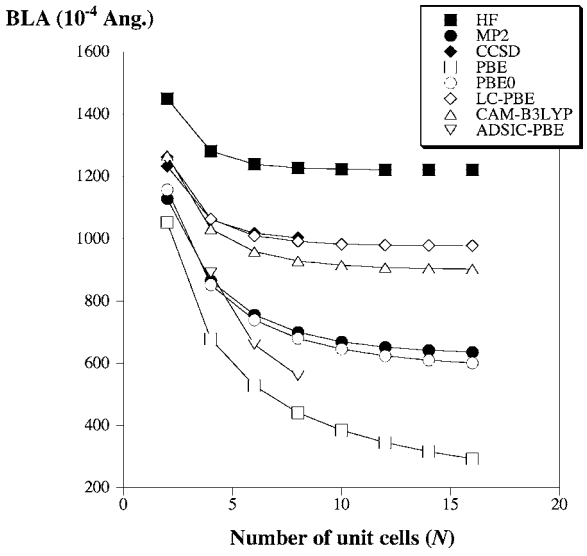

FIG. 2. Evolution with chain length of the BLA of all-*trans* polyacetylene.

TABLE II. BLA of PMI chains in the all-*trans* conformation. All values are in Å and have been computed with the 6-31G(*d*) basis set.

		N								
Method		2	4	6	8	10	12	14	16	Ref.
Ψ	HF	0.1558	0.1385	0.1294	0.1238	0.1195	0.1163	0.1137	0.1117	20
	MP2	0.1322	0.1119	0.1030	0.1000	0.0985	0.0975	0.0967	0.0960	74
	CCSD	0.1421	0.1281	0.1216	0.1188					This work
	CCSD(T)	0.1356	0.1181							65
LDA	SVWN5	0.1166	0.0837	0.0662	0.0564	0.0497	0.0447	0.0407	0.0374	65
GGA	BLYP	0.1311	0.0970	0.0789	0.0685	0.0616	0.0564	0.0523	0.0489	64
	PBE	0.1257	0.0917	0.0738	0.0637	0.0568	0.0517	0.0476	0.0442	64
LR	LC-BLYP	0.1439	0.1263	0.1172	0.1123	0.1086	0.1061	0.1041	0.1023	This work
	LC-PBE	0.1399	0.1217	0.1125	0.1075	0.1039	0.1011	0.0988	0.0971	This work
	CAM-B3LYP	0.1426	0.1214	0.1108	0.1048	0.1005	0.0972	0.0944	0.0922	This work
Hybrids	B3LYP	0.1359	0.1078	0.0934	0.0854	0.0799	0.0757	0.0721	0.0691	20
	PBE0	0.1333	0.1061	0.0923	0.0847	0.0793	0.0751	0.0717	0.0685	20

$$\Delta\alpha_L(N) = \frac{\alpha_L(N) - \alpha_L(N-2)}{2}, \tag{11}$$

that removes most of the chain end effects and leads to a fast convergence towards the asymptotic limit ($N \to \infty$). The polymeric responses have been obtained by extrapolating the oligomeric values as detailed in Ref. 66.

The electronic absorption spectra of dyes are computed by means of the TD-DFT methodology that provides the low-lying excited state energies. For the conjugated structures presented here, we report the longest wavelength of maximal absorption (λ_{max}) that presents a typical $\pi \to \pi^\star$ character associated with a large oscillator force. As the experimental UV/vis spectra are measured in solution, we have included surrounding effects in our simulations.[67–69] In this contribution, the bulk solvent effects are evaluated by means of the polarizable continuum model (PCM),[70] in which the solute lies inside a cavity, and the solvent is represented as a structureless material, characterized by macroscopic properties. PCM gives a valid approximation of the solvent effects, provided no specific solute-solvent interactions are present. Because we study UV/vis spectra, we have selected the nonequilibrium PCM solutions for the TD-DFT calculations.[71] The default PCM procedure has been used except for the anionic dyes (CYA-7, in Fig. 1) for which it was necessary to switch on the *noAddSph* and *radii=uaks* options in order to get convergence to the given thresholds. The *uaks* radii have been especially designed for the PBE0 functional. When the *addSph* (*noAddSph*) option is selected, extra spheres smoothing the surface cavity are (not) added. It is not expected to significantly affect the computed λ_{max}.

III. RESULTS

A. Bond length alternation

1. Polyacetylene

For PA, Mintmire and White have been the first to show that the DFT-LDA is unable to correctly predict the BLA: it was too small by a factor of 3 for the infinitely long chains,[17] as will also be confirmed later (see Ref. 18 and references therein). Choi *et al.* systematically studied the geometry of long PA oligomers using the B3LYP functional.[16] It turned out that HF overshoots the BLA by a factor of 2, whereas a pure GGA (BLYP) leads to the opposite misjudgment. In contrast, the MP2 and B3LYP geometries are both in good agreement with, on the one hand, higher-order electron-correlation methods and, on the other hand, with available experimental measurements for short oligomers.[16] More recently, Scuseria and co-workers noted that meta-GGA functionals do not correct significantly nor systematically the GGA BLA.[72,73] On the contrary, the inclusion of self-interaction corrections through KLI or ADSIC schemes provides a significant improvement for medium-sized chains.[27] Therefore, PA is the typical polymer for which the BLA is incorrectly (correctly) given by pure DFT functionals (traditional hybrids).[19]

In Table I, we compare the BLA of short and long all-*trans* PA oligomers obtained with LC-BLYP, LC-PBE, and CAM-B3LYP to the results from other DFT and wave function schemes. A graphical comparison is displayed in Fig. 2. These calculations have been performed with the 6-31G(*d*) atomic basis set. Despite its small size, this basis set provides accurate BLA estimates for both DFT and MP2 calculations.[16,19,20,73,74] For instance, the difference between the MP2/6-31G(*d*) and MP2/cc-pVDZ polymeric BLAs is limited to 0.002 Å.[73] For the octamer ($N=8$), the difference between the MP2/6-31G(*d*) and MP2/6-311G(3*df*) BLAs is only 0.003 Å.[74] Even with CCSD(T), going from 6-31G(*d*) to 6-311G(3*df*) only yields a 0.002 Å increase of the butadiene's BLA. Therefore, there is no doubt that 6-31G(*d*) is adequate in the present case. As expected, one finds in Table I an oscillating behavior when going up in the electron-correlation level included in wave-function-based theories. As a consequence, CCSD(T) BLAs are bracketed by the MP2 (low) and CCSD (high) results. From Fig. 2, it is striking that GGA and, to a smaller extent, ADSIC-GGA values are too small and decrease too rapidly as the chain lengthens, whereas MP2 and PBE0 curves are very similar. The same is

TABLE III. Comparison between the BLA obtained for PMI in the gliding-plane conformation. All values are in Å. The 6-31G(*d*) basis set is used but for ADSIC (DZP basis set).

		N								
Method		2	4	6	8	10	12	14	16	Ref.
Ψ	HF	0.1512	0.1290	0.1209	0.1144	0.1103	0.1069	0.1045	0.1024	65
	MP2	0.1285	0.1085	0.1042	0.1008	0.0991	0.0976	0.0965	0.0957	65
	CCSD	0.1395	0.1211	0.1166						This work
LDA	SVWN5	0.1069	0.0702	0.0588	0.0501	0.0439	0.0381	0.0331	0.0284	65
GGA	BLYP	0.1223	0.0890	0.0771	0.0633	0.0609	0.0548	0.0495	0.0446	65
	PBE	0.1162	0.0822	0.0706	0.0615	0.0549	0.0490	0.0439	0.0390	65
LR	LC-BLYP	0.1336	0.1082	0.1007	0.0994	0.0941	0.0899	0.0848	0.0827	This work
	LC-PBE	0.1291	0.1027	0.0952	0.0889	0.0848	0.0814	0.0790	0.0768	This work
	CAMB3LYP	0.1342	0.1082	0.0998	0.0929	0.0885	0.0846	0.0813	0.0792	This work
SIC	ADSIC-LDA	0.1661	0.1123	0.0902	0.0845		0.0780			65
Hybrids	B3LYP	0.1287	0.0991	0.0887	0.0804	0.0744	0.0692	0.0650	0.0610	65
	PBE0	0.1333	0.1061	0.0923	0.0847	0.0793	0.0751	0.0717	0.0685	65

true for the LC-PBE and CCSD lines. This means that LC-GGA provides a tremendous (and fast) improvement to the standard GGA scheme for the BLA of PA chains. Of course, LC-PBE and CCSD BLAs are likely to be slightly too large, but the results are still compatible with experimental polymeric data (0.08±0.03 Å).[73] Actually, CAM-B3LYP yields BLA in between the MP2 and CCSD results at all *N* and is probably the most interesting *ab initio* method ever tested for BLA of PA, with regard to its advantageous accuracy/computational effort balance. The main difference between CAM and LC is the speed of convergence: between $N=6$ and $N=10$ the BLA decreases by −0.0030 Å for LC-BLYP and by −0.0056 Å for CAM-B3LYP. This result is consistent with the maximal 100% (65%) HF exchange in LC (CAM).[53] Eventually, it is worth to highlight that selecting a BLYP or PBE GGA in the LC framework has a relatively small impact (typical variation of 0.0035 Å).

2. Polymethineimine

Polymethineimine, a polymer isoelectronic to PA where half of the CH groups are replaced by nitrogen atoms (Fig. 1), is a more challenging structure as, in this case, even full-range exchange hybrid functionals dramatically fail for the BLA.[20,64,65] Indeed, B3LYP and PBE0 provide much too small BLA for long chains. In Tables II and III the BLA for all-*trans* and gliding-plane conformers are, respectively, provided. For the all-*trans*, CCSD and CCSD(T) values are reported, whereas for the gliding plane that actually corresponds to the global minimum, ADSIC BLAs have recently been determined. At the MP2 and DFT levels of approximation it can be concluded from our previous tests that as for PA, 6-31G(*d*) is adequate.[64,65,74] As seen in Table II, one finds the same behavior for the wave function results as in the PA case: the CCSD BLAs are in between the HF and MP2 figures whereas the CCSD(T) BLAs are bracketed by the MP2 and CCSD values. For all-*trans* PMI, the evolution is sketched in Fig. 3. The LC and CAM schemes provide BLA in much better agreement with MP2, CCSD, and CCSD(T) than PBE, BLYP, B3LYP, and PBE0. For instance, the BLA for $N=10$ is 0.0985 Å with MP2, 0.1086 Å with LC-BLYP, 0.1005 Å with CAM-B3LYP, 0.0616 Å with BLYP, and 0.0799 Å with B3LYP. However, with regard to the MP2 and CCSD curves, one notes that both the LC and CAM BLAs are too rapidly decreasing with chain length: the MP2 and CAM-B3LYP (LC-PBE) curves cross for $N=12$ ($N=16$) (see Fig. 3). From $N=10$ to $N=16$, the MP2 BLA is decreased by −0.0025 Å, whereas CAM-B3LYP (LC-BLYP) BLA significantly overestimates the effect by −0.0083 Å (−0.0063 Å). Nevertheless, these errors are smaller than with B3LYP (−0.0108 Å) or BLYP (−0.0127 Å) functionals. This can be phenomenologically explained as, contrary to PA, the HF BLAs of PMI are also decreasing too rapidly (−0.0078 Å between $N=10$ and $N=16$): adding HF exchange cannot

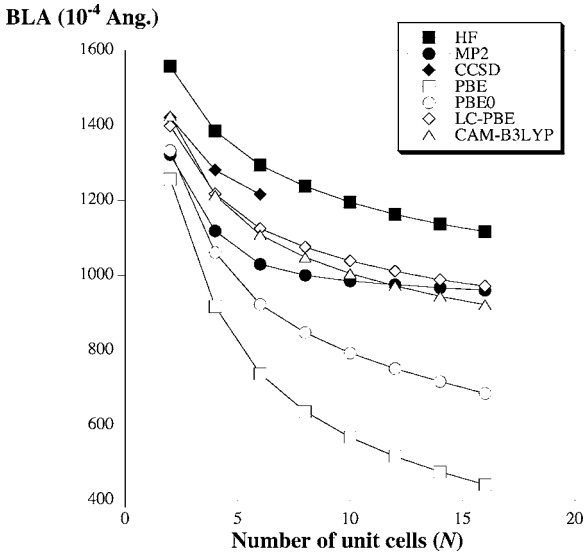

FIG. 3. Evolution with chain length of the BLA of all-*trans* polymethineimine.

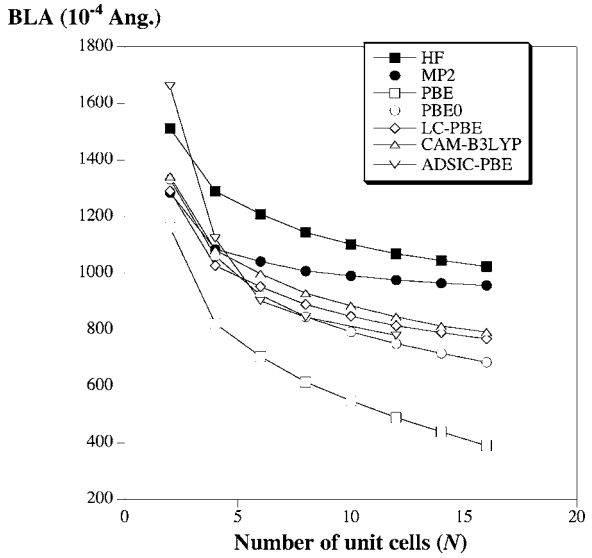

FIG. 4. Evolution with chain length of the BLA of gliding-plane polymethineimine.

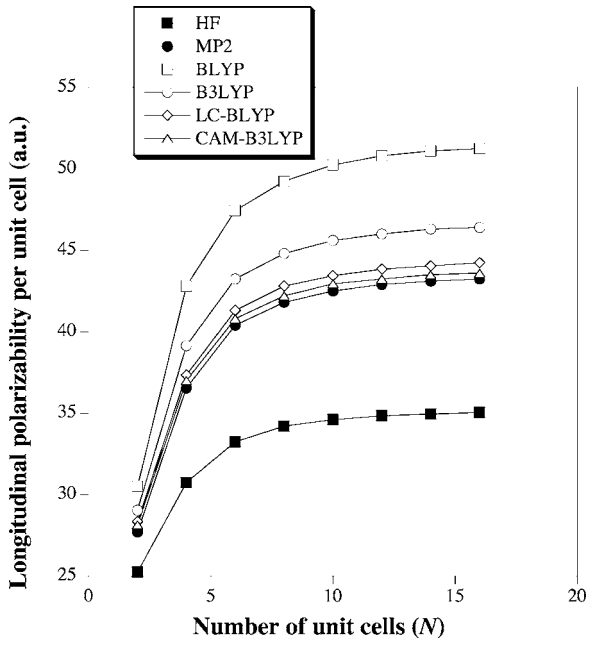

FIG. 5. Static longitudinal polarizability per unit cell $[\Delta\alpha(N)]$ for polyphosphazene chains.

completely erase GGA's limitations. For chains with a gliding-plane symmetry (Fig. 4), LC and ADSIC schemes provide similar BLAs provided $N \geqslant 6$. Though LC, CAM, and ADSIC moderate the incorrect evolution of the BLA obtained with GGA and traditional hybrid, they still provide too close bond lengths in comparison to MP2 and CCSD methodologies. In this particular case, HF provides BLA in good agreement with MP2 for long N, whereas pure DFT still yields much too small BLA. Therefore any "simple" mixing cannot be completely satisfying.

B. Polarizabilities

1. Polyphosphazene

We have computed the polarizability of *trans-cis* PPh chains based on the $PH_2{=}N$ unit cell (Fig. 1). Our results are shown in Table IV and have been evaluated with the same basis set as in Ref. 75. PPh and its derivatives constitute one of the most important class of inorganic polymers,[76] as they can be integrated into nonlinear optics (NLO) devices.[77] In this polymer, the electronic delocalization is moderate and can be rationalized with the so-called island model: the electrons "move" only over three adjacent atoms (PNP).[78] This moderate electronic mobility explains the quite small longitudinal polarizability per unit cell in comparison to the π-conjugated PA.[75] A more methodological consequence is that full-range exchange hybrid DFT functionals provide reasonable estimates for the polarizability of PPh. Indeed, for $N=16$ the PBE0 value is 671.6 a.u., only 5% above the MP2 result. The evolution with chain length of the polarizability per unit cell, $\Delta\alpha_L$, is sketched in Fig. 5. As expected for increasingly long compounds,[75,79–84] $\Delta\alpha_L$ rapidly increases with chain length for short oligomers, then enters a saturation regime where it tends toward the asymptotic value characterizing the infinite polymer. Pure GGAs obviously overestimate the $\Delta\alpha_L$ whereas the inclusion of LC provides polarizabilities in very good agreement with the reference MP2 values. The same is true with the CAM-B3LYP approach that is very satisfying in this case. In fact, for PPh, LR-DFT produces $\Delta\alpha_L$ in better agreement with electron-correlated wave function results than the traditional hybrids, similarly to the BLA of PA. Note that the α_L computed with BLYP and PBE are similar and become almost identical when the LC correction is applied.

2. Polymethineimine

The evolution with chain length of the polarizability and polarizability per unit cell of all-*trans* PMI oligomers can be

TABLE IV. Longitudinal static dipole polarizability of increasingly long *trans-cis* polyphoshphazene oligomers. All values are in a.u. and have been computed with the 6-31G(*d*) basis set on the HF/6-31G(*d*) geometry. A description of the geometries can be found in Ref. 75.

N	HF	MP2	BLYP	PBE	B3LYP	PBE0	LC-BLYP	LC-PBE	CAM-B3LYP
2	50.5	55.4	61.0	61.2	58.1	57.6	56.7	56.7	56.3
4	112.0	128.5	146.6	147.4	136.4	134.9	131.4	131.5	130.3
6	178.5	209.3	241.5	243.0	222.9	220.2	214.0	214.0	211.9
8	246.9	292.9	340.0	342.3	312.5	308.5	299.6	299.4	296.3
10	316.1	377.9	440.5	443.5	403.7	398.3	386.5	386.2	382.2
12	385.8	463.7	542.1	545.9	495.7	489.0	474.2	473.8	468.7
14	455.7	549.9	644.3	648.8	588.3	580.2	562.3	561.8	555.7
16	525.8	636.4	746.8	752.2	681.1	671.6	650.8	650.1	642.9

TABLE V. Longitudinal static dipole polarizability of all-*trans* polymethineimine chains. All values are in a.u. and have been computed with the 6-31G(*d*) basis set on the HF/6-31G(*d*) geometry (see Ref. 64). The HF, MP2, B3LYP, and PBE0 results come from Ref. 64. At the bottom of the table, the extrapolated values per unit cell of the polymer ($\infty \pm \Delta\infty$) are given.

N	HF	MP2	BLYP	PBE	B3LYP	PBE0	LC-BLYP	LC-PBE	CAM-B3LYP
2	57.1	52.6	59.0	58.7	57.8	57.4	56.1	55.8	56.7
4	159.5	148.7	186.6	185.9	176.1	173.5	160.6	160.0	165.8
6	294.1	283.2	392.4	391.1	354.3	345.8	304.4	303.2	318.8
8	448.3	445.6	670.1	669.0	579.9	561.6	474.5	472.7	503.2
10	614.9	628.5	1010.9	1008.4	840.5	808.9	662.8	660.2	709.1
12	790.0	826.6	1398.8	1395.8	1126.3	1078.6	864.1	860.8	930.4
14	970.9	1036.0	1821.1	1817.7	1430.4	1364.8	1075.0	1070.8	1163.2
16	1156.0	1254.2	2266.9	2263.2	1748.1	1663.3	1293.0	1288.0	1404.4
18	1344.1	1478.9	2728.5	2724.4	2076.3	1971.4	1516.4	1510.5	1652.2
20	1534.6	1708.6	3201.5	3196.9	2412.9	2287.0	1743.9	1737.2	1905.0
22	1726.7	1942.2	3683.2	3678.1	2756.0	2608.5	1974.5	1966.9	2161.6
24	1920.1	2178.6	4172.2	4166.6	3104.4	2934.7	2207.5	2199.0	2421.1
26	2114.5	2417.3	4667.9	4661.8	3457.1	3264.6	2442.4	2433.1	2683.0
28	2309.6	2657.9	5169.5	5162.8	3813.2	3597.4	2678.7	2668.4	2946.6
30	2505.3	2899.8	5676.4	5669.2	4172.0	3932.7	2916.1	2905.0	3211.6
∞	99.7	126.1	281.5	280.5	188.7	178.3	122.4	120.8	136.6
$\Delta\infty$	1.8	4.1	20.5	19.5	9.2	3.8	2.0	3.7	4.4

found in Table V and Fig. 6, respectively. The MP4 and CCSD(T) α_L of the dimer and tetramer are within 1% of the MP2 results.[64] One can therefore trust MP2 α_L. The pure DFT approaches overshoot the α_L, the effect being even enhanced for long chains. Indeed, BLYP (PBE) α_L are larger than the MP2 values by 12% (12%) for $N=2$, by 61% (60%) for $N=10$, by 87% (87%) for $N=20$, and by 123% (122%) for $N=\infty$. Full-range exchange hybrids correct the phenomenon, but too weakly. Indeed, with B3LYP (PBE0), α_L are larger than the MP2 values by 10% (9%) for $N=2$, by 34% (29%) for $N=10$, by 41% (34%) for $N=20$, and by 50% (41%) for $N=\infty$. On the contrary, the LC-GGAs are on the spot: the differences are negligible at all *N*. For the dimer (polymer), LC-BLYP and LC-PBE α_L are larger (smaller) than MP2 figures by 7% and +6% (−3% and −4%), respectively. CAM-B3LYP α_L are bracketed by LC-BLYP and B3LYP (+8% for $N=2$, +13% for $N=10$, +12% for $N=20$, and +8% for $N=\infty$). As a consequence, the LC-GGA $\Delta\alpha_L$ in Fig. 6 are slightly larger than the MP2 values for short *N* and slightly smaller for long *N*, though the overall agreement is really stunning. In the same framework, CAM-B3LYP is slightly less accurate. Yet, it significantly improves the evolution with chain length given by B3LYP and PBE0. For oligoenes[56] and push-pull oligoenes,[30] the agreement between LC-DFT and electron-correlated schemes is not so impressive, but compared to GGA, the description of the evolution with chain length is nicely improved. This clearly demonstrates that LR-DFT is able to consistently (at all *N*) remove the exploding error phenomena induced by GGA, whereas B3LYP and PBE0 functionals only moderate these exaggeration trends.

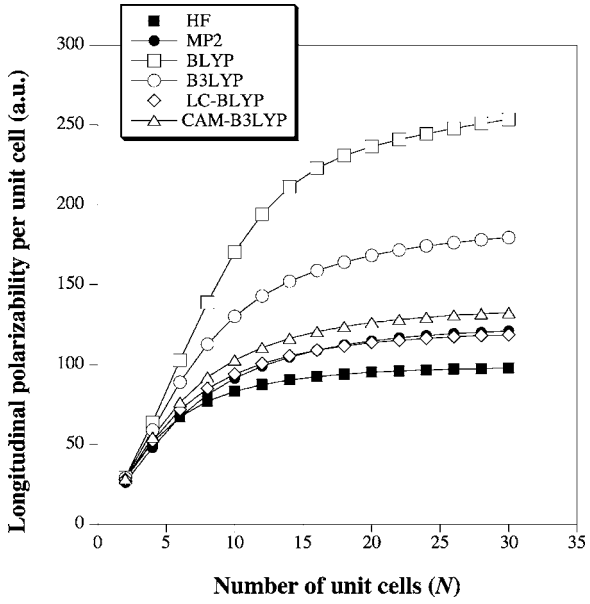

FIG. 6. Static longitudinal polarizability per unit cell [$\Delta\alpha(N)$] for polymethineimine chains.

C. Absorption spectra

1. Anthraquinones

9,10-anthraquinone derivatives (AQ, Fig. 1) are one of the most important classes of industrial dyes (30% of today's world production).[85] AQ in which the central ring bearing two carbonyl groups is fused to two fully aromatic six-member rings can give rise to a complete range of shades (especially in the green/blue region), depending on the nature and relative position(s) of the auxochromic group(s) substituting hydrogen atom(s) on the outer rings.[85,86] One can therefore find several experimental data for the λ_{max} of AQ dyes.[85–87] For AQ, we have recently demonstrated that a PCM-TD-DFT approach combined to B3LP/PBE0 functionals can be very efficient in reproducing the experimental trends, even with relatively small basis sets.[88–90] Indeed, for 66 AQs, we obtained mean absolute errors (MAEs) of 20 nm (0.12 eV) and 14 nm (0.08 eV) with B3LYP and PBE0,

TABLE VI. λ_{max} (in nm) for a series of anthraquinones. These results are obtained with the PCM-TD-X/6-311++G(d,p)//B3LYP/6-311G(d,p) approach in CH_2Cl_2. Experimental values are from Ref. 87; B3LYP and PBE0 λ_{max} are from Ref. 88. At the bottom of the table, the mean signed error (MSE, in nm) for nonfitted data, the linear expt./theory correlation coefficient (R^2), as well as the mean absolute error (MAE, in nm) computed before and after linear fitting are reported.

	X								
Substitution	HF	BLYP	PBE	B3LYP	PBE0	LC-BLYP	LC-PBE	CAM-B3LYP	Expt.
2-OH	249.7	477.6	476.5	400.1	383.6	324.5	321.8	341.2	365
1-OH	289.3	479.9	478.9	411.2	396.6	346.6	345.2	358.6	405
2-NH_2	300.1	571.6	571.0	464.8	443.4	358.9	356.1	381.8	410
1,2-OH	294.2	522.2	522.2	437.9	421.0	354.6	353.7	371.5	416
1,5-OH	299.6	503.5	502.2	432.9	417.1	361.6	360.1	375.6	428
1,8-OH	301.8	508.3	507.3	437.7	420.1	369.4	368.6	380.8	430
2,3-NH_2	310.3	637.8	640.8	504.6	480.0	372.5	371.7	401.6	442
1-NH_2	324.3	564.8	562.9	480.3	462.6	393.8	392.4	411.2	465
1,4-OH	332.9	528.4	529.7	467.2	454.1	405.6	405.5	416.0	476
1,2-NH_2	321.7	583.5	584.1	497.7	475.0	394.6	394.1	415.3	480
1,5-NH_2	330.7	572.5	567.8	490.1	472.2	401.4	400.1	420.0	480
1,8-NH_2	337.4	616.2	616.1	517.7	497.5	421.1	419.9	439.8	492
1,4-NH_2	396.6	591.0	591.1	539.0	526.3	472.2	472.3	485.6	550
1,4,5,8-NH_2	422.6	678.6	679.1	602.4	586.7	521.5	522.1	536.4	610
MSE (no fit)	−138.4	99.1	98.6	16.8	−0.9	−67.9	−69.0	−51.0	
MAE (no fit)	138.4	99.1	98.6	20.7	15.3	67.9	69.0	51.0	
R^2	0.99	0.60	0.77	0.88	0.91	0.98	0.99	0.98	
MAE (fit)	7.6	28.8	28.9	16.2	13.8	4.8	5.6	7.2	

respectively.[88] In Table VI, we report the 6-311++G(d,p) transition energies for 14 representative hydroxy and amino AQs solvated in dichloromethane. These calculations have been performed on a gas-phase B3LYP/6-311G(d,p) geometry as the rigidity of the AQ core impedes significant modifications of the geometrical parameters in solution.[89] Previous to any fitting, PBE0 has the edge with both the smallest mean signed error (MSE) and MAE. Consistently with our previous investigations,[88,89] B3LYP yields a quite similar MAE. On the contrary, HF wavelengths are always too small (by 138 nm on average) whereas BLYP and PBE wavelengths suffer the opposite drawback (by 99 nm on average). The LC procedure corrects the too small transition energies predicted by pure GGA, but to a too large amount: the LC-DFT λ_{max} are too short by about 68–69 nm. As expected, CAM decreases the B3LYP λ_{max} by a smaller extent but also leads to a systematic overestimation of the excitation energies (51 nm). This is illustrated in Fig. 7. If one uses a simple linear fitting (SLR) procedure to correct the raw TD-DFT (and TD-HF) figures, one gets a very poor correlation (R^2) for both GGA (BLYP: 0.60, PBE: 0.77), significantly improved with traditional hybrids (B3LYP: 0.88, PBE0: 0.91), and tremendously better for the LR-DFT (at least 0.98). Accidentally, this is also the case with TD-HF (R^2: 0.99). Therefore, though the absolute λ_{max} provided by LC-BLYP, LC-PBE, and CAM-B3LYP are significantly less accurate than the B3LYP and PBE0 figures, the former models allow a more consistent description of the substitution effects. In fact, after a SLR fit the LC-BLYP MAE is smaller than 5 nm, a highly valuable result that cannot be obtained with B3LYP or PBE0, even after a more refined statistical treatment.[88] Such success can be partly attributed to the unexpected qualitative consistency of the HF approximation in the present case.

2. Cyanine dyes

Cyanine derivatives are cationic or anionic dyes that can be found with a large variety of lengths and chain ends.[91] There are the prototype examples, for which TD-DFT completely fails to reproduce the experimental evolution of the λ_{max} with increasing N.[23,24,92] A quite deceiving result in-

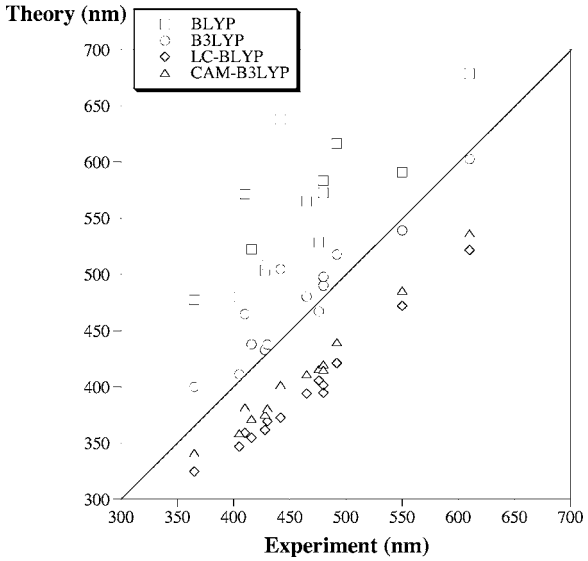

FIG. 7. Comparison between theoretical and experimental λ_{max} (in nm) for substituted AQ dyes. The central line indicates a perfect theory/experiment match.

TABLE VII. Wavelength (in nm) of the first dipole-allowed electronic transition of model cyanine chains (Fig. 1). The same method is used for both the 6-311G(d,p) ground-state optimizations and the 6-311++G(d,p) transition energies calculations. The CAS-PT2 values correspond to the CAS-PT2(4s3p2d/2s1p)//B3LYP/6-31G(d,p) wavelengths given in Ref. 92.

			X							
Series	*N*	CAS-PT2	HF	BLYP	PBE	B3LYP	PBE0	LC-BLYP	LC-PBE	CAM-B3LYP
CYA-1	0	191	146	171	168	164	161	166	163	163
	1	290	215	243	240	236	232	239	236	235
	2	390	275	310	306	301	297	306	303	300
	3	492	330	370	365	360	355	368	365	360
	4	588	381	426	422	415	410	427	423	416
	5		428	481	475	468	462	483	479	469
CYA-2	0		128	134	132	132	130	130	128	130
	1		199	227	224	219	215	215	213	215
	2		251	296	292	284	279	276	273	276
	3		298	357	352	342	336	332	329	332
	4		340	413	409	396	390	383	380	384
	5		377	469	463	448	440	430	427	434
CYA-3	0		146	171	168	164	161	166	163	163
	1		237	267	263	260	256	266	262	260
	2		307	348	344	339	335	349	345	339
	3		365	423	419	409	404	421	416	409
	4		409	498	493	477	470	487	482	473
	5		437	575	570	543	534	546	541	534
CYA-4	0		128	134	132	132	130	130	128	130
	1		199	227	224	219	215	215	213	215
	2		255	312	307	297	291	287	283	287
	3		303	390	385	368	360	350	346	353
	4		343	466	461	436	426	406	402	412
	5		374	543	537	501	489	455	450	467

deed, as for cyanine the simple electron in the box approximation works pretty well.[93] In Table VII, we report gas-phase λ_{max} for four series of cyanines (symmetric/asymmetric, all-*trans*/ *cis-trans*). For the all-*trans* symmetric series, CYA-1, GGA, traditional hybrids, and LR functionals provide nearly the same transition energies at all N. While all DFT approaches do agree, they are in strong disagreement with the CAS-PT2 values by Schreiber *et al.*[92] It appears that the DFT transition wavelengths are too small and too slowly increasing with N: for N=4, the difference between CAS-PT2 and DFT results is close to 150 nm, and LC and CAM models do not help, probably due to the qualitative inadequacy of the monodeterminantal approaches. Indeed, it has been shown that when the chain lengthens the excitation loses its simple one-electron character and corresponds to a significant mixing of states.[92] For the asymmetric series, CYA-2, the effects of LC and CAM are slightly larger but the computed λ_{max} does not strongly differ from the figures obtained with full-range exchange hybrids. Totally similar conclusions can be drawn for the *cis-trans* series (CYA-3 and CYA-4). The N=2 CYA-4 has been treated by Chiba *et al.*[34] with the 6-31G(d) basis set. They obtained λ_{max} of 303 nm Becke exchange (B) + one-parameter progressive (OP) correlation (BOP), a GGA, 290 nm (B3LYP), and 281 nm (LC-BOP), in good agreement with our 6-311++G(d,p) results. For that system, the difference between the LC and GGA λ_{max} increases with chain length (88 nm for N=5), but unfortunately it seems that the correction is going in the wrong direction (decreasing the wavelength instead of increasing it). In Table VIII, the solvated transition energies for synthesized cyanine derivatives bearing positive or negative charges are reported and compared to experimental values. The same phenomena as in Table VII clearly appear: (i) the differences between LC, CAM, and traditional hybrid results are quite negligible, (ii) the DFT λ_{max} are too small and tend to decrease too slowly with chain length, and (iii) CAS-PT2 provides results in much better agreement with experiment. At this stage, one has therefore to conclude that the TD-DFT framework fails to reproduce quantitatively or qualitatively the absorption spectra of cyanine dyes, whatever the functional (GGA, traditional hybrid, LC, etc.) selected.

IV. CONCLUSIONS AND OUTLOOK

We have applied a long-range corrected DFT approach to the computation of properties of large conjugated systems, that are often incorrectly predicted by conventional DFT approaches relying on pure and/or full-range exchange hybrid functionals. In all cases, the form of the GGA (BLYP or PBE) included in the LR-DFT procedure has only a marginal impact on the result accuracy. LC-DFT and CAM-B3LYP provide bond length alternations of polyacetylene oligomers

TABLE VIII. Wavelength (in nm) of the first dipole-allowed electronic transition of cyanine chains (Fig. 1). All calculations have been performed with the PCM-TD-X/6-311++G(d,p)//PCM-X/6-311G(d,p) model. All experimental values are from Ref. 91 and references therein.

			X								
Series	Solvent	*N*	HF	BLYP	PBE	B3LYP	PBE0	LC-BLYP	LC-PBE	CAM-B3LYP	Expt.
CYA-1[a]	Water	1	222	254	250	247	242	250	246	245	286
		2	287	329	325	319	315	325	320	318	378
CYA-5	MeOH	1	230	272	270	261	256	261	258	257	296
		2	296	345	341	333	328	336	333	330	395
		3	357	414	410	402	396	411	407	400	493
CYA-6[b]	DCM	0	175	224	225	210	207	205	204	203	224
		1	235	286	285	272	268	269	267	266	313
		2	305	362	360	348	343	349	346	343	416
		3	370	433	430	418	413	418	414	408	519
CYA-7	MeOH	0	258	337	342	313	307	303	301	300	346
		1	316	402	400	378	372	371	369	366	440
		2	378	454	451	446	438	444	441	436	540
		3	437	518	514	510	502	517	513	503	632

[a]Gas-phase CAS-PT2 values: 290 nm (N=1) and 390 nm (N=2). See Ref. 92.
[b]Gas-phase CAS-PT2 values: 297 nm (N=1), 420 nm (N=2), and 534 nm (N=3). See Ref. 92.

in very good agreement with high-order electron-correlation wave function approaches. For polymethineimine, LR-DFT significantly improves the (poor) description given by the traditional hybrids but tends to overestimate the rate of the BLA decrease when the chain lengthens. The evolution with chain length of the polarizability per unit cell of both polyphosphazene and polymethineimine is perfectly reproduced by LC-GGA, the agreement with MP2 results being really astonishing. This confirms previous results.[30,33] CAM-B3LYP also provides much more accurate polarizabilities than B3LYP. For substituted anthraquinones, the CAM and LC approaches significantly overestimate the main transition energy and are therefore unable to reproduce the accuracy of B3LYP and PBE0. On the contrary, after a statistical treatment, LR-DFT yields very accurate λ_{max}, i.e., the auxochromic shifts are consistently predicted. For both model and realistic cyanine dyes, LR-DFT does not cure the incorrect absorption spectrum evolution with chain length. Although LC-DFT is based on a more consistent and appealing physical model than the fitted-error compensation of most traditional hybrids, it still practically relies on a HF/GGA error cancellation. Therefore, as for many hybrids, LC-DFT is most efficient when the discrepancies given by HF and GGA evolve with opposite trends. For cyanines, both HF and GGA predict excitation energies that are decreasing (much) too slowly with chain length, and LR-DFT is ineffective. This is probably related to the nonmonodeterminantal character of the excitation process. Of course, for most chemical properties, B3LYP and PBE0 still remain efficient and affordable solutions for (TD-)DFT calculations, and switching to LR-DFT is only relevant for difficult issues.

We are currently investigating other classes of organic chromophores with TD-LR-DFT approaches in order to assess the suitability of such procedures for determining the color of dyes.

ACKNOWLEDGMENTS

Two of the authors (D.J. and E.A.P.) thank the Belgian National Fund for their research associate positions. Three of the authors (D.J., E.A.P., and C.A.) thank the Commissariat Général aux Relations Internationale for supporting this work within the framework of the Tournesol Scientific cooperation between the Communauté Française de Belgique and France. Non LR-DFT calculations have been performed on the Interuniversity Scientific Computing Facility (ISCF), installed at the Facultés Universitaires Notre-Dame de la Paix (Namur, Belgium), for which the authors gratefully acknowledge the financial support of the FNRS-FRFC and the "Loterie Nationale" for Convention No. 2.4578.02, and of the FUNDP.

[1] J. P. Perdew, A. Ruzsinsky, J. Tao, V. N. Staroverov, G. E. Scuseria, and G. I. Csonka, J. Chem. Phys. **123**, 062001 (2005).
[2] A. D. Becke, J. Chem. Phys. **98**, 5648 (1993).
[3] C. Adamo and V. Barone, J. Chem. Phys. **110**, 6158 (1999).
[4] M. Ernzerhof and G. E. Scuseria, J. Chem. Phys. **110**, 5029 (1999).
[5] C. Adamo and V. Barone, J. Chem. Phys. **108**, 664 (1998).
[6] J. P. Perdew, M. Ernzerhof, and K. Burke, J. Chem. Phys. **105**, 9982 (1996).
[7] F. A. Hamprecht, A. J. Cohen, D. J. Tozer, and N. C. Handy, J. Chem. Phys. **109**, 6264 (1998).
[8] H. L. Schmider and A. D. Becke, J. Chem. Phys. **108**, 9624 (1998).
[9] W. M. Hoe, A. J. Cohen, and N. C. Handy, Chem. Phys. Lett. **341**, 319 (2001).
[10] A. D. Boese and N. C. Handy, J. Chem. Phys. **116**, 9559 (2002).
[11] V. N. Staroverov, G. E. Scuseria, J. Tao, and J. P. Perdew, J. Chem. Phys. **119**, 12129 (2003).
[12] A. D. Boese and J. M. L. Martin, J. Chem. Phys. **121**, 3405 (2004).
[13] X. Xu and W. A. Goddard III, Proc. Natl. Acad. Sci. U.S.A. **101**, 2673 (2004).
[14] T. W. Keal and D. J. Tozer, J. Chem. Phys. **123**, 121103 (2005).
[15] Y. Zhao and D. G. Truhlar, J. Phys. Chem. A **108**, 6908 (2004).
[16] C. H. Choi, M. Kertesz, and A. Karpfen, J. Chem. Phys. **107**, 6712 (1997).
[17] J. W. Mintmire and C. T. White, Phys. Rev. B **35**, 4180 (1987).
[18] J. Paloheimo and J. von Boehm, Phys. Rev. B **46**, 4304 (1992).

[19] D. Jacquemin, E. A. Perpète, I. Ciofini, and C. Adamo, Chem. Phys. Lett. **405**, 376 (2005).
[20] D. Jacquemin, A. Femenias, H. Chermette, I. Ciofini, C. Adamo, J. M. André, and E. A. Perpète, J. Phys. Chem. A **110**, 5952 (2006).
[21] B. Champagne, E. A. Perpète, S. van Gisbergen, E. J. Baerends, J. G. Snijders, C. Soubra-Ghaoui, K. Robins, and B. Kirtman, J. Chem. Phys. **109**, 10489 (1998).
[22] B. Champagne, E. A. Perpète, D. Jacquemin, S. van Gisbergen, E. Baerends, C. Soubra-Ghaoui, K. Robins, and B. Kirtman, J. Phys. Chem. A **104**, 4755 (2000).
[23] D. Guillaumont and S. Nakamura, Dyes Pigm. **46**, 85 (2000).
[24] J. Fabian, Theor. Chem. Acc. **106**, 199 (2001).
[25] D. J. Tozer, J. Chem. Phys. **119**, 12697 (2003).
[26] A. Dreuw and M. Head-Gordon, J. Am. Chem. Soc. **126**, 4007 (2004).
[27] I. Ciofini, C. Adamo, and H. Chermette, J. Chem. Phys. **123**, 121102 (2005).
[28] O. V. Gritsenko and E. J. Baerends, J. Chem. Phys. **121**, 655 (2004).
[29] Y. Tawada, T. Tsuneda, S. Yanagisawa, T. Yanai, and K. Hirao, J. Chem. Phys. **120**, 8425 (2004).
[30] M. Kamiya, H. Sekino, T. Tsuneda, and K. Hirao, J. Chem. Phys. **122**, 234111 (2005).
[31] N. T. Maitra, J. Chem. Phys. **122**, 234104 (2005).
[32] F. A. Bulat, A. Toro-Labbé, B. Champagne, B. Kirtman, and W. Yang, J. Chem. Phys. **123**, 014319 (2005).
[33] H. Iikura, T. Tsuneda, T. Yanai, and K. Hirao, J. Chem. Phys. **115**, 3540 (2001).
[34] M. Chiba, T. Tsuneda, and K. Hirao, J. Chem. Phys. **124**, 144106 (2006).
[35] J. B. Krieger, Y. Li, and G. J. Iafrate, Phys. Rev. A **45**, 101 (1992).
[36] G. Vignale and W. Kohn, Phys. Rev. Lett. **77**, 2037 (1996).
[37] C. Legrand, E. Suraud, and P. G. Reinhard, J. Phys. B **35**, 1115 (2002).
[38] M. van Faasen, P. L. Boeij, R. van Leeuwen, J. A. Berger, and J. G. Snijders, Phys. Rev. Lett. **88**, 186401 (2002).
[39] I. Ciofini, H. Chermette, and C. Adamo, Chem. Phys. Lett. **380**, 12 (2003).
[40] M. van Faasen, P. L. Boeij, R. van Leeuwen, J. A. Berger, and J. G. Snijders, J. Chem. Phys. **118**, 1044 (2003).
[41] A. Savin, in *Recent Developments and Applications of Modern Density Functional Theory*, edited by J. M. Seminario (Elsevier, Amsterdam, 1996), Chap. 9, pp. 327–354.
[42] T. Leininger, H. Stoll, H. J. Werner, and A. Savin, Chem. Phys. Lett. **275**, 151 (1997).
[43] W. Yang and Q. Wu, Phys. Rev. Lett. **89**, 143002 (2002).
[44] T. Yanai, D. P. Tew, and N. C. Handy, Chem. Phys. Lett. **393**, 51 (2004).
[45] J. Toulouse, F. Colonna, and A. Savin, Phys. Rev. A **70**, 062505 (2004).
[46] T. Yanai, R. J. Harrison, and N. C. Handy, Mol. Phys. **103**, 413 (2005).
[47] B. Champagne, F. A. Bulat, W. Yang, S. Bonness, and B. Kirtman, J. Chem. Phys. **125**, 194114 (2006).
[48] M. J. G. Peach, T. Helgaker, P. Salek, T. W. Keal, O. B. Lutnaes, D. J. Tozer, and N. C. Handy, Phys. Chem. Chem. Phys. **8**, 558 (2006).
[49] J. Heyd, G. E. Scuseria, and M. Ernzerhof, J. Chem. Phys. **118**, 8207 (2003).
[50] N. T. Maitra and D. G. Tempel, J. Chem. Phys. **125**, 184111 (2006).
[51] O. A. Vydrov and G. E. Scuseria, J. Chem. Phys. **125**, 234109 (2006).
[52] D. Y. Wang, Q. Ye, B. G. Li, and G. L. Zhang, Nat. Prod. Res. **17**, 365 (2003).
[53] E. Rudberg, P. Salek, T. Helgaker, and H. Agren, J. Chem. Phys. **123**, 184108 (2005).
[54] T. Sato, T. Tsuneda, and K. Hirao, Mol. Phys. **103**, 1151 (2005).
[55] Z. L. Cai, M. J. Crossley, J. R. Reimers, R. Kobayashi, and R. D. Amos, J. Phys. Chem. B **110**, 15624 (2006).
[56] H. Sekino, Y. Maeda, and M. Kamiya, Mol. Phys. **103**, 2183 (2005).
[57] R. Kobayashi and R. D. Amos, Chem. Phys. Lett. **420**, 106 (2006).
[58] R. D. Adamson, J. P. Dombroski, and P. M. W. Gill, Chem. Phys. Lett. **254**, 329 (1996).
[59] A. D. Becke, Phys. Rev. A **38**, 3098 (1988).
[60] C. Lee, W. Yang, and R. G. Parr, Phys. Rev. B **37**, 785 (1988).
[61] J. P. Perdew, K. Burke, and M. Ernzerhof, Phys. Rev. Lett. **77**, 3865 (1996).
[62] M. J. Frisch, G. W. Trucks, H. B. Schlegel *et al.*, GAUSSIAN 03, Revision C.02, Gaussian, Inc., Wallingford, CT, 2004.
[63] M. J. Frisch, G. W. Trucks, H. B. Schlegel *et al.*, GAUSSIAN DVP, Revision E.05, Gaussian, Inc., Wallingford, CT, 2006.
[64] D. Jacquemin, J. M. André, and E. A. Perpète, J. Chem. Phys. **121**, 4389 (2004).
[65] D. Jacquemin, E. A. Perpète, H. Chermette, I. Ciofini, and C. Adamo, Chem. Phys. **332**, 79 (2007).
[66] B. Champagne, D. Jacquemin, J. M. André, and B. Kirtman, J. Phys. Chem. A **101**, 3158 (1997).
[67] J.-F. Guillemoles, V. Barone, L. Joubert, and C. Adamo, J. Phys. Chem. A **106**, 11354 (2002).
[68] L. Petit, C. Adamo, and N. Russo, J. Phys. Chem. B **109**, 12214 (2005).
[69] A. D. Quartarolo, N. Russo, and E. Sicilia, Chem.-Eur. J. **12**, 6797 (2006).
[70] J. Tomasi, B. Mennucci, and R. Cammi, Chem. Rev. (Washington, D.C.) **105**, 2999 (2005).
[71] M. Cossi and V. Barone, J. Chem. Phys. **115**, 4708 (2001).
[72] K. N. Kudin and G. E. Scuseria, Phys. Rev. B **61**, 16440 (2000).
[73] R. Pino and G. Scuseria, J. Chem. Phys. **121**, 8113 (2004).
[74] D. Jacquemin, A. Femenias, H. Chermette, J. M. André, and E. A. Perpète, J. Phys. Chem. A **109**, 5734 (2005).
[75] D. Jacquemin, O. Quinet, B. Champagne, and J. M. André, J. Chem. Phys. **120**, 9401 (2004).
[76] H. R. Allcock, *Chemistry and Applications of Polyphosphazenes* (Wiley, New York, 2002).
[77] H. R. Allcock, R. Ravikiran, and M. A. Olshavsky, Macromolecules **31**, 5206 (1998).
[78] H. R. Allcock, Chem. Rev. (Washington, D.C.) **72**, 315 (1972).
[79] G. J. B. Hurst, M. Dupuis, and E. Clementi, J. Chem. Phys. **89**, 385 (1988).
[80] B. Kirtman, Chem. Phys. Lett. **143**, 81 (1988).
[81] B. Champagne, D. H. Mosley, and J. M. André, J. Chem. Phys. **100**, 2034 (1994).
[82] J. L. Toto, T. T. Toto, C. P. de Melo, B. Kirtman, and K. A. Robins, J. Chem. Phys. **104**, 8586 (1996).
[83] D. Jacquemin, B. Champagne, and B. Kirtman, J. Chem. Phys. **107**, 5076 (1997).
[84] D. Jacquemin, E. A. Perpète, and J. M. André, J. Chem. Phys. **120**, 10317 (2004).
[85] F. J. Green, *The Sigma-Aldrich Handbook of Stains, Dyes and Indicators* (Aldrich Chemical, Milwaukee, WI, 1990).
[86] R. H. Thomson, *Naturally Occurring Quinones*, 2nd ed. (Academic, London, 1971).
[87] H. Labhart, Helv. Chim. Acta **152**, 1410 (1957).
[88] E. A. Perpète, V. Wathelet, J. Preat, C. Lambert, and D. Jacquemin, J. Chem. Theory Comput. **2**, 434 (2006).
[89] D. Jacquemin, J. Preat, M. Charlot, V. Wathelet, J. M. André, and E. A. Perpète, J. Chem. Phys. **121**, 1736 (2004).
[90] D. Jacquemin, J. Preat, V. Wathelet, J. M. André, and E. A. Perpète, Chem. Phys. Lett. **405**, 429 (2005).
[91] J. Fabian and H. Hartmann, *Light Absorption of Organic Colorants*, Reactivity and Structure Concepts in Organic Chemistry Vol. 12 (Springer-Verlag, Berlin, 1980).
[92] M. Schreiber, V. Bub, and M. P. Fülscher, Phys. Chem. Chem. Phys. **3**, 3906 (2001).
[93] H. Kuhn, J. Chem. Phys. **17**, 1198 (1949).